Chiral symmetry in Quarkyonic matter

Toru Kojo[1,*]

[1] *RIKEN BNL Research Center, Brookhaven National Laboratory, USA*

The $1/N_c$ expansion classifies nuclear matter, deconfined quark matter, and Quarkyonic matter in low temperature region. We investigate the realization of chiral symmetry in Quarkyonic matter by taking into account condensations of chiral particle-hole pairs. It is argued that chiral symmetry and parity are locally violated by the formation of chiral spirals, $\langle\bar{\psi}\exp(2i\mu_q z\gamma^0\gamma^z)\psi\rangle$. An extension to multiple chiral spirals is also briefly discussed.

1. QUARKYONIC MATTER

Quantum Chromodynamics (QCD) at high baryon density and low temperature has attracted continuous interests [1]. Recently large N_c [2] arguments raised conceptual questions in dense QCD [3]. It turns out that a transition scale from nuclear to quark matter ($\mu_q \sim \Lambda_{\rm QCD}$) and that of deconfinement ($\mu_q \sim \sqrt{N_c}\Lambda_{\rm QCD}$) are, *at least conceptually*, different. The phase where quark density is sufficiently high to form the quark Fermi sea, nevertheless excitations are confined, is called *Quarkyonic* phase [3–6].

To characterize Quarkyonic matter, below we will first distinguish nuclear matter and quark matter, and then classify quark matter into deconfined quark matter and Quarkyonic matter. The $1/N_c$ expansion will be used for theoretical classifications. The schematic phase diagram based on the $1/N_c$ expansion is shown in Fig. 1.

Nuclear matter starts to appear slightly below the threshold of nucleons, $\mu_q = M_N/N_c \sim \Lambda_{\rm QCD}$, and changes into the quark matter within a small variation $\sim 1/N_c^2$ in a quark chemical potential[1]. Let us first see how nuclear matter descriptions violate in higher density, and then consider why quark matter picture becomes reasonable descriptions.

* Electronic address: torujj@quark.phy.bnl.gov

[1] Actually, this argument implicitly assumes that nuclear forces in large N_c behave in a qualitatively similar way as those of $N_c = 3$ world. This view is not commonly accepted, however. Attempts to construct nucleons which provide nuclear forces similar to those of $N_c = 3$ can be found in Ref. [7].

When nucleons are treated as basic degrees of freedom, change in μ_q requires large change of the nucleon Fermi momentum k_F, since k_F is divided by a large mass in kinetic energy $\sim k_F^2/M$. Accordingly a number density of nucleons $\sim k_F^3$ increases rapidly, and nucleons start to overlap, then strong nuclear forces in short distance become relevant. In such a region, it is natural to change effective degrees of freedom from nucleons to quarks for which interactions are weaker in shorter distance. This is the reason why it is much more reasonable to apply the picture of the quark Fermi sea, instead of the nucleon Fermi sea. Here quarks need not belong to particular nucleons since strongly overlapped nucleons can maintain color singletness. A 1st order like rapid growth of quark density characterizes transitions from hadronic-nuclear to quark matter. The large $N_{\rm c}$ limit provides clear distinction between nuclear and quark matters.

Now let us discuss properties of the quark Fermi sea. Quarks deeply inside of the Fermi sea are perturbative, since Pauli blocking prevents them from being affected by small momentum transfer processes. Such quarks share a large fraction of the Fermi sea, so perturbative estimates should reasonably work for bulk quantities such as pressure to which all quarks contribute. On the other hand, small momentum transfer processes can affect quarks near the Fermi surface. Although such quarks have large momenta $\sim \mu_q$, they find comoving quarks with which they exchange small momenta, generating nonperturbative phenomena. They play deterministic roles for the phase structure (since perturbative contributions are common to different phases), transport processes, which are sensitive to excitation properties near the Fermi surface. The schematic picture is summarized in Fig. 2.

Now a question is how such a soft interaction looks like at finite density. In the QCD vacuum, quantum fluctuations of gluons provide confinement, while those of quarks screen gluons reducing confining effects. The strength of fluctuations can be roughly characterized by a number of degrees of freedom: $O(N_{\rm c}^2)$ for gluons, and $O(N_{\rm c})$ for quarks. At finite density, an allowed phase space for low momentum $q\bar{q}$ excitations increases, so do screening effects. The perturbative estimate of the screening scale is $\sim g_s^2\mu_q^2 \sim \mu_q^2/N_{\rm c}$, which becomes comparable with $\Lambda_{\rm QCD}$ when $\mu_q \sim \sqrt{N_{\rm c}}\Lambda_{\rm QCD}$. This is the scale, where deconfinement takes place. The estimate provided here may be minimal, since any energy gaps of quarks are not taken into account: Mass gaps from Lorentz vector self-energy (chiral symmetric) and possible chiral symmetry breaking would suppress $q\bar{q}$ excitations with reducing screening effects.

It might sound strange to speak about confinement in the region, where quarks are already released from nucleons. To draw a qualitative picture, let us consider quarks in terms of quantum wavefunctions. Quarks occupy states in a color singlet way, forming a color white background. A quark excitation in such a background inevitablly accompanies a colored quark-hole, and they are confined forming a mesonic state. Glueballs are also confined, and their spectra are discrete without multi-gluon continuum. The dominant baryonic excitations are presumably baryon number solitons which are coherent excitations of quarks and quark-holes which keep the color singletness together with the background – there is no clear separation of baryons from the background. A correction to this simple argument comes from colored fluctuations in a color white background, which are already addressed in terms of screening effects.

These arguments can be tested by studying 1+1 dimensional QCD which is a confining model. At finite density, the strength of confinement is unchanged irrespective of how closely quarks are packed within one spatial dimensional line. This is because screening effects at finite density are always same as those in vacuum, due to the same allowed phase space for $q\bar{q}$ fluctuations [8].

Finally it should be emphasized that we have not used a notion of chiral symmetry breaking/restoration to define Quarkyonic matter. Quarkyonic matter is solely defined by the presence of the quark Fermi sea and confined excitations. Their consequences on chiral symmetry are discussed in the next section.

2. LOCAL VIOLATION OF THE CHIRAL SYMMETRY: QUARKYONIC CHIRAL SPIRALS

As μ_q increases, the conventional particle-antiparticle type chiral condensate disappears since generations of antiparticles need large energies $\sim \mu_q$ to transfer particles in the Dirac sea to the above of the Fermi sea (Fig. 3). Yet chiral symmetry can be broken by chiral pairs of particles and holes near the Fermi surface without costing much energy. Chiral condensates of this sort only employ particle-holes near the Fermi surface, modifying only particle dispersions around there. This is consistent with arguments on perturbative quarks deeply inside of the Fermi sea.

For simplicity, only typical two cases, exciton and density wave types, will be considered

below (for detail, see [8]). In the exciton case, we pick up a particle and a hole from the same spatial momentum region. Since a hole momentum must be flipped, the pair has a total momentum ~ 0. For the density wave, we pick up a particle and a hole from the opposite momentum region, so the pair has a total momentum $\sim 2\mu_q$, forming nonuniform condensates. Such situations have been first discussed in [9], in the context of deconfined quark matter.

Since we pick up a particle and a hole with similar kinetic energies in both cases, main differences in pairing energies come from potentials. The confining potential should provide a big difference. We expect that exciton wavefunctions made of pairs with opposite large momenta are widely spread in space, costing large energies due to long strings. For density wave pairs, particles and holes comove together maintaining small sizes of $\sim 1/\Lambda_{\rm QCD}$. Therefore we naively expect that confining forces favor density wave pairings.

We first consider the one-pair problem picking up particle-hole from $p_z \sim \pm\mu_q,\ p_T \sim 0$. This setup will turn out to be a good starting point to analyze multi-pair problems [10].

For concrete arguments, we introduce a simple model of the linear confinement in which gluon propagators take the following form (screening effects are suppressed in large $N_{\rm c}$),

$$D_{44}^{AB}(k) = -\frac{8\pi}{C_F} \times \frac{\sigma}{(\mathbf{k}^2)^2}\,\delta^{AB} \quad ; \quad D^{4i} = D^{ij} = 0\ , \quad (C_F = \frac{N_{\rm c}^2-1}{2N_{\rm c}},\ \sigma \sim \Lambda_{\rm QCD}^2) \qquad (1)$$

which shows a linear potential in coordinate space. This model is inspired by Coulomb gauge analyses [11]. We have omitted perturbative parts for the sake of simplicity [12].

To investigate condensations, we analyze self-consistent equations by reducing 3+1 dimensional equations to 1+1 dimensional ones (the essence was already discussed in [13]). Below we illustrate this for the Schwinger-Dyson equation for the quark self-energy. It looks like

$$\not{\Sigma}(p) + \Sigma_m(p) = -\int \frac{d^4k}{(2\pi)^4}\,(\gamma_4 t_A)\,S(k;\Sigma)\,(\gamma_4 t_B)\,D_{44}^{AB}(p-k)\ , \qquad (2)$$

where the quark propagator is dressed and depends on $\Sigma(p)$. We will investigate the self-energy for quarks near the Fermi surface, with $p_z \sim \mu_q$ and $p_T \sim 0$.

Three points are relevant for the dimensional reduction: (I) Our gluon propagator behaves as $1/(\mathbf{q}^2)^2$, so dominant contributions of the integral (3) sharply concentrates on the small domain. (II) Different Dirac structures $S(k) = \gamma_4 S_4(k) + \gamma_z S_z(k) + \gamma_T \cdot \mathbf{S}_T(k) + S_m(k)$, give the ratio of $|S_T|/S_z \sim k_T/k_z \sim \Lambda_{\rm QCD}/\mu_q$, so we can drop off S_T and Σ_T in the leading order of $\Lambda_{\rm QCD}/\mu_q$. (III) The quark energy is sensitive to change of k_z while not to that of

k_T. Change in k_T is along the constant energy surface which looks flat for $\Lambda_{\rm QCD}/\mu_q \ll 1$, without changing the quark energy a lot.

Because of the restricted integral region and the insensitivity of the quark propagator to k_T variable, we can set $\mathbf{k}_T \simeq \mathbf{0}_T$ and factorize the integral equation:

$$\int dk_4 dk_z d^2\mathbf{k}_T \; S(k_4, k_z, \mathbf{k}_T)\; D_{44}(p-k) \;\rightarrow \int dk_4 dk_z \; S(k_4, k_z, \mathbf{0}_T) \int d\mathbf{k}_T \; D_{44}(p-k), \quad (3)$$

for which we can carry out the $\mathbf{k}_T$ integral. The smearing of gluon propagator yields a 1+1 dimensional confining propagator, $\sim 1/(p_z - k_z)^2$. The reduced equation then becomes

$$\bar{\not{\Sigma}}(p_4, p_z, \mathbf{0}_\perp) + \Sigma_m(p_4, p_z, \mathbf{0}_\perp) \simeq \frac{N_{\rm c} g_{\rm 2D}^2}{2} \int \frac{dk_4\, dk_z}{(2\pi)^2}\; \gamma_4\; \bar{S}(k_4, k_z, \mathbf{0}_\perp)\; \gamma_4\; \frac{1}{(k_z - p_z)^2}\;, \quad (4)$$

where $N_{\rm c} g_{\rm 2D}^2 = 4\sigma$ and we denote $\bar{\Sigma}, \bar{S}$ for components other than transverse ones. The resulting equation is nothing but the Schwinger-Dyson equation of 't Hooft model in axial gauge $A_z = 0$. The same approximations are applicable to the Bethe-Salpeter equation.

Since self-consistent equations for our one-pair problem take the same form as those of 't Hooft model [14], we can borrow results in the existing literatures [15]. Only nontrivial issues are relationships between 3+1 and 1+1 dimensional operators and condensation channels. In particular, concepts of spins are absent in one spatial dimension. In our dimensional reduction, the tranverse part of the quark propagators are suppressed. This implies that $\boldsymbol{\gamma}_T$ terms are dropped off, so that there is no spin mixing term once we quantize spins along the directions of moving particles. Introducing projection operators for moving directions, we can write spin multiplets [13],

$$\psi_\pm = \frac{1 \pm \gamma^0\gamma^z}{2}\psi\;, \qquad \varphi_\uparrow = \begin{bmatrix} \varphi_{\uparrow+} \\ \varphi_{\uparrow-} \end{bmatrix} = \begin{bmatrix} \psi_{R+} \\ \psi_{L-} \end{bmatrix} \quad ; \quad \varphi_\downarrow = \begin{bmatrix} \varphi_{\downarrow+} \\ \varphi_{\downarrow-} \end{bmatrix} = \begin{bmatrix} \psi_{L+} \\ \psi_{R-} \end{bmatrix}\;, \quad (5)$$

where indices $(+,-)$ for $+z$,$-z$ moving particles. Let us introduce 1+1 dimensional "flavor", $\Phi^T \equiv (\varphi_\uparrow, \varphi_\downarrow)$, and Dirac matrices, $\Gamma^0 = \sigma^1$, $\Gamma^z = -i\sigma^2$, $\Gamma^5 = \sigma^3$. Then 3+1 dimensional quark bilinears without spin mixings are mapped onto 1+1 dimensional "flavor" *singlet* operators [8, 13],

$$\bar\psi\psi \rightarrow \bar\Phi\Phi, \qquad \bar\psi\gamma^0\psi \rightarrow \bar\Phi\Gamma^0\Phi, \qquad \bar\psi\gamma^z\psi \rightarrow \bar\Phi\Gamma^z\Phi, \qquad \bar\psi\gamma^0\gamma^z\psi \rightarrow \bar\Phi\Gamma^5\Phi. \quad (6)$$

The last relation reflects the fact that 1+1 dimensional Γ^5 characterizes moving directions. All other quark bilinears include spin mixings, so they are "flavor" *non-singlet* in 1+1 dimensions. They do not show condensations in 't Hooft model.

It is known that chiral spirals, $\langle\bar{\Phi}e^{2i\mu_q z\Gamma^5}\Phi\rangle$, appear in 1+1 dimensions, so that we get the chiral spiral in 3+1 dimensions by using the above dictionary,

$$\langle\bar{\psi}\psi\rangle = \Delta\cos(2\mu_q z), \quad \langle\bar{\psi}\gamma^0\gamma^z\psi\rangle = \Delta\sin(2\mu_q z). \tag{7}$$

An origin of this chiral rotation is that $\bar{\psi}_+\psi_-$ and $\bar{\psi}_-\psi_+$ moving to opposite directions each other, thus have opposite phase $e^{\pm 2i\mu_q z}$; this phase mismatch makes $\langle\bar{\psi}\gamma^0\gamma^z\psi\rangle = \langle\bar{\psi}_+\psi_-\rangle - \langle\bar{\psi}_-\psi_+\rangle$ nonvanishing. So the chiral density wave accompanies its partner, forming spiral structures.

It is clear that a spatial average of chiral condensates vanishes because of spatial modulations. So the symmetry apparently looks restored for probes with large wavelength. Note also that our chiral tensor type condensate locally breaks parity (Fig. 4).

Finally we briefly mention an extension of the present results to those of multi-pairs. This problem was investigated in [10]. A key observation is that in confining models, chiral spirals evolved in different spatial directions interact only weakly. Therefore our results for one-patch problem may be applied with slight modifications. Such a picture indicates that a number of directions of chiral spiral formations increases as μ_q, with a series of phase transitions (Fig. 5).

3. SUMMARY AND OUTLOOK

In quarkyonic phase, excitations are confined despite of large quark number density. They drive the formation of the chiral spirals with large mass gaps $\sim \Lambda_{\rm QCD}$. This is in sharp contrast to the situation in deconfined quark matter, where gaps are too small to overtake screening effects [13]. Indeed, both of gaps and screening masses are induced by density effects, and screening masses develop faster and larger than gaps. In contrast, the main origin of Quarkyonic chiral spirals is the confining force rather than density effects themselves. This is also seen in the fact that the magnitude of condensates does not involve μ explicitly. Quarkyonic chiral spirals can appear before screening effects fully develop.

So Quarkyonic chiral spirals can be regarded as good signatures peculiar to Quarkyonic phase. They break translational invariance, chiral symmetry and parity locally. Accordingly several Goldstone modes appear as low energy excitations near the Fermi surface. They are relevant in the transport processes in Quarkyonic matter. Also, as suggested in NJL model

studies [16, 17], the presence of inhomogeneous phases may provide significant impacts on the critical point search in experiments and in lattice QCD.

ACKNOWLEDGMENTS

The author acknowledges his collaborators, Y. Hidaka, L. McLerran, R. D. Pisarski, and A. M. Tsvelik with whom ideas presented here have been developed. This research is supported under DOE Contract No. DE-AC02-98CH10886 and Special Posdoctoral Research Program of RIKEN. He also thanks organizers at JINR for their warm hospitality.

---

1. For a recent review, K. Fukushima and T. Hatsuda, Rep. Prog. Phys. **74**, 014001 (2011).
2. G. 't Hooft, Nucl. Phys. B **72**, 461 (1974).
3. L. McLerran and R. D. Pisarski, Nucl. Phys. A **796**, 83 (2007).
4. L. McLerran, K. Redlich, and C. Sasaki, Nucl. Phys. A **824**, 86 (2009).
5. A. Andronic *et al.*, Nucl. Phys. A **837**, 65 (2010).
6. Y. Hidaka, L. D. McLerran, and R. D. Pisarski, Nucl. Phys. A **808**, 117 (2008).
7. Y. Hidaka, T. Kojo, L. D. McLerran, and R .D. Pisarski, to be published in Nucl. Phys. A.
8. T. Kojo, Y. Hidaka, L. McLerran, and R. D. Pisarski, Nucl. Phys. A **843**, 37 (2010), and references therein.
9. D. V. Deryagin, D. Y. Grigoriev, and V. A. Rubakov, Int. J. Mod. Phys. A **7**, 659 (1992).
10. T. Kojo, R. D. Pisarski, and A. M. Tsvelik, Phys. Rev. D **82**, 074015 (2010).
11. D. Zwanziger, Phys. Rev. Lett. **90**, 102001 (2003); Phys. Rev. D **69**, 016002 (2004).
12. L. Ya. Glozman, R. F. Wagenbrunn, Phys. Rev. **D 77**, 054027 (2008).
13. E. Shuster and D. T. Son, Nucl. Phys. B **573**, 434 (2000).
14. G. 't Hooft, Nucl. Phys. B **75**, 461 (1974).
15. B. Bringoltz, Phys. Rev. D **79**, 125006 (2009).
16. D. Nickel, Phys. Rev. Lett. **103**, 072301 (2009).
17. S. Carignano, D. Nickel, and M. Buballa, Phys. Rev. D **82**, 054009 (2010).

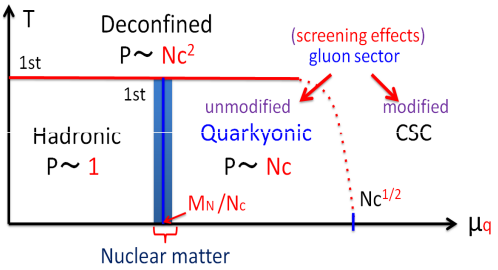

Figure 1. A schematic phase diagram based on the $1/N_c$ expansion. Hadronic, deconfined, and quark matter are separated by (approximate) first order phase transition lines. Quark matter is further devided into Quarkyonic matter and conventional quark matter with deconfined excitations. The deconfined quark matter is expected to be the color superconducting (CSC) phase. Nuclear matter exists only around the boundary between hadronic and quark matter.

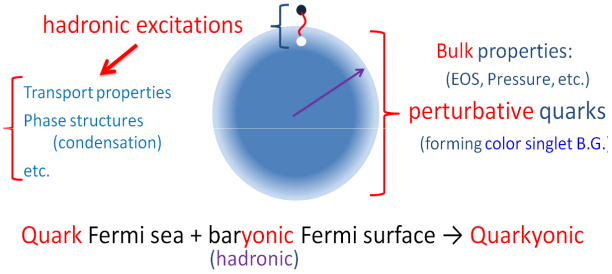

Figure 2. The quark Fermi sea in Quarkyonic matter. Most of quarks in the Fermi sea are nearly perturbative, while quarks near the Fermi surface are nonperturbatively affected. The colored states strongly interact one another, and only colorless combinations can appear as physical excitations.

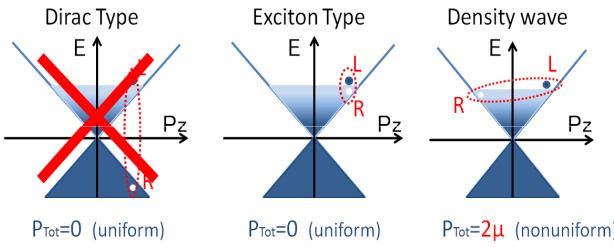

Figure 3. Three typical candidates which break the chiral symmetry. The Dirac type condensate is made of quarks and anti-quarks, while other two candidates are made of quarks and quark-holes. The creation of anti-quarks cost large energy of $O(\mu)$, so can be neglected.

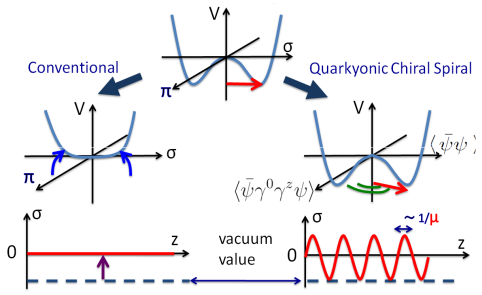

Figure 4. The chiral restoration phenomena. The conventional chiral restoration requires vanishing chiral condensates everywhere, while in Quarkyonic matter, only spatial average of condensates becomes zero. The condensate $\langle\bar{\psi}\gamma^0\gamma^z\psi\rangle$ also breaks parity locally.

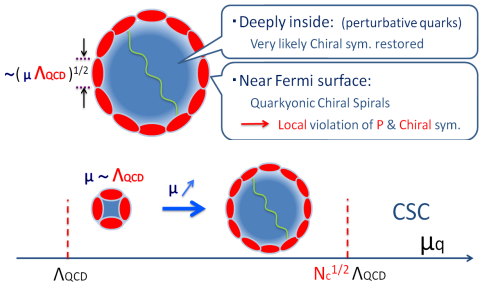

Figure 5. A schematic picture on chiral symmetry in Quarkyonic matter. Deeply inside of the Fermi sea, quarks have little chance to feel non-perturbative effects, and chiral symmetry breaking effects are weak. Near the Fermi surface, confining forces drive chiral symmetry breaking. A number of chiral spirals increases as density does. Eventually confining forces are screened, and the amplitudes of chiral spirals disappear.

FIGURE CAPTIONS

Fig.1: A schematic phase diagram based on the $1/N_c$ expansion. Hadronic, deconfined, and quark matter are separated by (approximate) first order phase transition lines. Quark matter is further devided into Quarkyonic matter and conventional quark matter with deconfined excitations. The deconfined quark matter is expected to be the color superconducting (CSC) phase. Nuclear matter exists only around the boundary between hadronic and quark matter.

FIG.2: The quark Fermi sea in Quarkyonic matter. Most of quarks in the Fermi sea are nearly perturbative, while quarks near the Fermi surface are nonperturbatively affected. The colored states strongly interact one another, and only colorless combinations can appear as physical excitations.

Fig.3: Three typical candidates which break the chiral symmetry. The Dirac type condensate is made of quarks and anti-quarks, while other two candidates are made of quarks and quark-holes. The creation of anti-quarks cost large energy of $O(\mu)$, so can be neglected.

Fig.4: The chiral restoration phenomena. The conventional chiral restoration requires vanishing chiral condensates everywhere, while in Quarkyonic matter, only spatial average of condensates becomes zero. The condensate $\langle\bar{\psi}\gamma^0\gamma^z\psi\rangle$ also breaks parity locally.

Fig.5: A schematic picture on chiral symmetry in Quarkyonic matter. Deeply inside of the Fermi sea, quarks have little chance to feel non-perturbative effects, and chiral symmetry breaking effects are weak. Near the Fermi surface, confining forces drive chiral symmetry breaking. A number of chiral spirals increases as density does. Eventually confining forces are screened, and the amplitudes of chiral spirals disappear.